ORNL-5354

cy. 1

Elevated-Temperature Tensile Properties of ERNiCr-3 Weld Metal

R. L. Klueh
J. F. King

[redacted]

OAK RIDGE NATIONAL LABORATORY
CENTRAL RESEARCH LIBRARY
CIRCULATION SECTION
4500N ROOM 175
LIBRARY LOAN COPY
DO NOT TRANSFER TO ANOTHER PERSON
If you wish someone else to see this report, send in name with report and the library will arrange a loan.
UCN 7969 3 9-77

OAK RIDGE NATIONAL LABORATORY
OPERATED BY UNION CARBIDE CORPORATION FOR THE ENERGY RESEARCH AND DEVELOPMENT ADMINISTRATION

Printed in the United States of America. Available from
the Department of Energy,
Technical Information Center
P.O. Box 62, Oak Ridge, Tennessee 37830
Price: Printed Copy $4.50; Microfiche $3.00

This report was prepared as an account of work sponsored by an agency of the United States Government. Neither the United States Government nor any agency thereof, nor any of their employees, contractors, subcontractors, or their employees, makes any warranty, express or implied, nor assumes any legal liability or responsibility for any third party's use or the results of such use of any information, apparatus, product or process disclosed in this report, nor represents that its use by such third party would not infringe privately owned rights.

ORNL-5354
Distribution
Category
UC-79b, -h, -k

Contract No. W-7405-eng-26

METALS AND CERAMICS DIVISION

ELEVATED-TEMPERATURE TENSILE PROPERTIES OF ERNiCr-3 WELD METAL

R. L. Klueh and J. F. King

Date Published - December 1977

OAK RIDGE NATIONAL LABORATORY
Oak Ridge, Tennessee 37830
operated by
UNION CARBIDE CORPORATION
for the
DEPARTMENT OF ENERGY

CONTENTS

ABSTRACT 1
INTRODUCTION 2
EXPERIMENTAL 3
RESULTS 4
Tensile Studies 4
Microstructure 12
DISCUSSION 20
SUMMARY AND CONCLUSIONS 28
ACKNOWLEDGMENTS 30
REFERENCES 30

ELEVATED-TEMPERATURE TENSILE PROPERTIES OF ERNiCr-3 WELD METAL*

R. L. Klueh and J. F. King

ABSTRACT

The filler metal alloy designated by AWS Specification as ERNiCr-3 and commonly known as Inconel 82 has a nominal composition of 67% Ni–20% Cr–3% Mn–3% Fe–2.5% Nb and is used conventionally to join austenitic-ferritic dissimilar-metal joints. Tensile properties were determined for this alloy over the range 25 to 732°C at strain rates of 3×10^{-4} and 3×10^{-6}/s. Specimens were taken from four different gas tungsten-arc weldments: three were 40-pass welds made between 19-mm-thick plates; one was a seven-pass weld between 13-mm-thick plates. Microprobe analyses of the two weldment geometries indicated that iron was the only element from the base metal that significantly diluted the weld metal. Considerably more dilution was found in the small weld than in the large one.

The tensile tests at 3×10^{-4}/s (most tests were at this strain rate) on the four welds indicated only minor data scatter for the ultimate tensile strength with somewhat more scatter for the yield strength. For the ultimate tensile strength, weldment size had no effect, while the yield strength of the small weldment fell below that for the larger weldments. Ductility was quite constant over the entire test temperature range: the total elongation ranged between 30 and 40% and the reduction of area between 40 and 60%. The uniform elongation decreased from about 30% at 25°C to less than 10% at 732°C.

Above about 454°C, both the yield strength and the ultimate tensile strength in the low-strain-rate tests showed significant increases over the strengths at the higher strain rate. The enhanced values for the yield strength persisted to the highest test temperature (732°C), whereas the ultimate tensile for the low strain rate fell below the curve for the higher strain rate at about 600°C. Above 600°C, the ultimate tensile strength dropped off rapidly, and at 677°C approached the yield strength (i.e., the uniform elongation dropped to less than 1%). The strain rate effects have been tentatively attributed to "K-state" formation, an effect that some investigators have attributed to short-range order formation in other Ni-Cr base alloys.

---

*Work performed under DOE/RDD 189a No. OH103, Piping and Fittings Development.

Optical microscopy of the as-deposited ERNiCr-3 indicated minor defects widely scattered through the material. These were judged to be small cracks or voids that were along grain boundaries and were undectable by radiography. Although all specimens appeared to fracture by a transgranular mode, scattered grain boundary cracks were observed in numerous fractured specimens.

INTRODUCTION

The intermediate heat exchanger of the Clinch River Breeder Reactor Plant (CRBRP) is to be constructed of an austenitic stainless steel and the steam generators from the low-alloy ferritic 2 1/4 Cr-1 Mo steel. Thus, a welded transition joint between these two units will be required. Since a number of joints of this type has failed in fossil-fired plants, we are presently developing transition weld procedures for the CRBRP steam generator circuit. Included in these studies will be the determination of the mechanical properties of filler metals and transverse weldments that are appropriate for such transition joints.

To make a transition joint between type 316 stainless steel and 2 1/4 Cr-1 Mo steel, the present procedure calls for the use of the filler metal designated by AWS as ERNiCr-3. This is a nickel alloy with approximately 20% Cr, several percent Fe, Mn, and Nb, and lesser amounts of several other elements. The chemical composition limits for the alloy are given in Table 1.

Table 1. Limiting Chemical Composition for ERNiCr-3[a]

Element	Content (wt %)	Element	Content (wt %)
Ni	67.0 min	Cu	0.50 max
C	0.10 max	Cr	18.0–22.0
Mn	2.5–3.5	Ti	0.75 max
Fe	3.0 max	Nb	2.0–3.0
S	0.015 max	Co	0.75 max
Si	0.50 max	P	0.03 max

[a]Specifications: ASTM B.304 (ERNiCr-3), AWS A5.14 (ERNiCr-3).

Because of the differences in thermal coefficient of expansion between the materials in such a joint, a transition piece is being considered. Instead the transition between type 316 stainless steel and 2 1/4 Cr-1 Mo steel being made directly with weld metal deposited from ERNiCr-3 filler wire, an intermediate spool piece of alloy 800 would be used. Regardless of whether such a transition piece is used or not, ERNiCr-3 filler metal will undoubtedly be used (between the alloy 800 and 2 1/4 Cr-1 Mo steel if a transition piece is used). For this reason, our first mechanical properties studies are being made on this weld metal.

Relatively few data are available for ERNiCr-3 weld metal. One manufacturer[1] gives data over the range 25 to 1090°C (75–2000°F) in a company bulletin on alloy 800. Payne[2] has reported almost identical data over the same temperature range.

EXPERIMENTAL

One problem with testing weld metal is the fabrication of sufficient welds to obtain the required number of specimens for the test program. Initially it was decided to make the ERNiCr-3 welds between two 13-mm-thick (1/2-in.) plates — one plate of alloy 800, the other of 2 1/4 Cr-1 Mo steel. A 90°-included-angle V-groove joint geometry was used. The welding was performed by the automatic gas tungsten-arc process with cold-wire filler additions. About seven passes were required to complete the weld. The nominal welding parameters were: 150 A and 10 V, with a travel speed of about 0.9 mm/s.

Since the number of specimens that could be obtained from such welds was quite limited, a larger weld was designed to produce a large deposit of ERNiCr-3 filler metal. Plates of 19-mm-thick (3/4-in.) 2 1/4 Cr-1 Mo steel were used as base material. These were prepared with a 30°-included-angle V-groove joint geometry with a 32-mm (1 1/4-in.) root opening and a backing strip. Weld deposits were also made by the automatic gas tungsten-arc welding process with cold-wire filler additions. Filling this joint required 40 weld passes; the welding parameters were the same as those used for the small weld.

Before specimens were machined, the welds were nondestructively examined by radiography. No defects could be detected. As a result of some premature creep failures early in the program, specimens were subsequently radiographed before being tested. In all cases, no defects were detected that would have caused the weld to be rejected. The radiographic technique used could detect defects of 0.075 to 0.13 mm (0.003–0.005 in.).

Mechanical property test specimens were of a buttonhead type with a 3.18-mm-diam (0.125-in.) and 28.6-mm-long (1.125-in.) gage section. The specimens tested were longitudinal all-weld-metal specimens. Tensile tests were made on an Instron machine with crosshead speeds of 8.5 and 0.085 μm/s (0.02 and 0.0002 in./min). Before test, all specimens were postweld heat-treated 1 hr at 732°C.

RESULTS

Tensile Studies

Detailed tensile studies were made over the range 25 to 732°C and a nominal strain rate of 3×10^{-4}/s (crosshead speed of 8.5 μm/s). Only one series of tests was made on the specimens taken from the 13-mm-thick plates (plate 1 of Table 2) before we decided to use weld metal from welds made on the 19-mm-thick plates so more test specimens could be obtained per weld. Specimens taken from three of the 19-mm-thick plates (plates 2, 3, and 4 of Table 2) were tested over the entire temperature range. Specimens from the welds on the 13-mm-thick plates were tested at 25, 454, 510, 566, and 621°C.

When the results from plates 1 and 2 (one 13-mm and one 19-mm) are compared (Table 2 and Fig. 1), significant differences in strength properties are noted — especially for the yield strength. Our initial conclusion from these results was that dilution effects for the different welds significantly affected the properties. As a result of that conclusion, we examined these welds for chemical composition changes, and these results will be discussed in the following section. However,

Table 2. Tensile Properties of ERNiCr-3 Weld Metal[a] at a Strain Rate[b] of 3.0×10^{-4}/s

Test Temperature		Strength, MPa (ksi)			Elongation, %		Reduction of Area
(°C)	(°F)	Yield	Ultimate	Fracture	Uniform	Total	(%)
			Plate 1				
25	77	295(42.9)	610(88.6)	483(70.1)	39.1	43.9	45.8
25	77	311(45.2)	622(90.3)	474(68.8)	33.3	37.6	44.4
454	850	219(31.8)	507(73.6)	442(64.1)	41.8	46.8	47.7
510	950	229(33.3)	488(70.8)	413(59.9)	35.8	38.9	40.0
566	1050	220(32.0)	478(69.4)	377(54.6)	39.2	43.0	51.6
621	1150	203(29.5)	421(61.3)	237(34.2)	32.8	38.0	47.0
			Plate 2				
25	77	335(51.3)	658(95.5)	476(69.1)	30.4	34.7	44.1
204	400	305(44.3)	575(83.4)	473(68.7)	34.3	36.7	45.6
316	600	298(43.2)	548(79.6)	452(65.6)	26.4	29.9	45.5
454	850	282(41.0)	542(78.7)	474(68.9)	36.8	40.6	43.7
510	950	267(38.8)	501(72.7)	369(53.5)	33.9	37.1	40.1
566	1050	259(37.6)	486(70.6)	371(53.9)	33.6	37.6	51.5
621	1150	258(37.4)	451(65.4)	265(38.4)	25.8	29.4	50.4
677	1250	256(37.1)	405(58.8)	62(9.0)[c]	15.3	19.0[c]	30.9[c]
677	1250	247(35.8)	422(61.2)	141(20.4)	19.9	28.3	46.9
732	1350	261(37.9)	327(47.2)	124(18.0)	4.1	29.9	53.7
			Plate 3				
25	77	339(49.2)	601(87.3)	476(69.1)	32.8	39.3	43.6
204	400	292(42.4)	557(80.8)	421(61.1)	35.1	40.2	47.0
316	600	264(38.3)	524(76.0)	355(51.5)	33.8	38.1	46.9
454	850	274(39.7)	490(71.1)	416(60.3)	32.7	36.3	45.8
510	950	258(37.4)	477(69.2)	388(56.3)	30.1	33.2	39.7
566	1050	240(34.8)	451(65.4)	347(50.4)	33.0	35.3	37.4
621	1150	251(36.5)	444(64.4)	101(14.7)	31.6	36.6	46.7
677	1250	236(34.3)	413(60.0)	130(18.8)	23.0	31.8	51.4
732	1350	228(33.1)	335(48.6)	85(12.3)	7.7	41.7	68.5
			Plate 4				
25	77	351(51.0)	618(89.7)	471(68.3)	36.2	40.7	59.1
204	400	262(38.0)	557(80.9)	449(65.1)	40.7	44.9	50.5
316	600	260(37.7)	535(77.6)	428(62.1)	36.6	40.5	49.8
454	850	249(36.2)	515(74.7)	431(62.6)	41.6	46.6	50.7
510	950	243(35.3)	493(71.6)	436(63.3)	40.4	44.6	57.2
566	1050	256(37.2)	465(67.5)	373(54.1)	33.7	37.1	51.6
621	1150	267(38.8)	449(65.2)	359(52.1)	28.6	32.7	49.0
677	1250	251(36.5)	422(61.2)	155(22.5)	22.2	33.6	55.6
732	1350	262(38.0)	338(49.0)	55(8.0)	6.7	39.8	42.2

[a]All specimens were postweld heat-treated for 1 hr at 732°C (1350°F).

[b]Tests were at a constant crosshead speed of 8.5 μm/s.

[c]Failed near end of gage section at point where extensometer was attached.

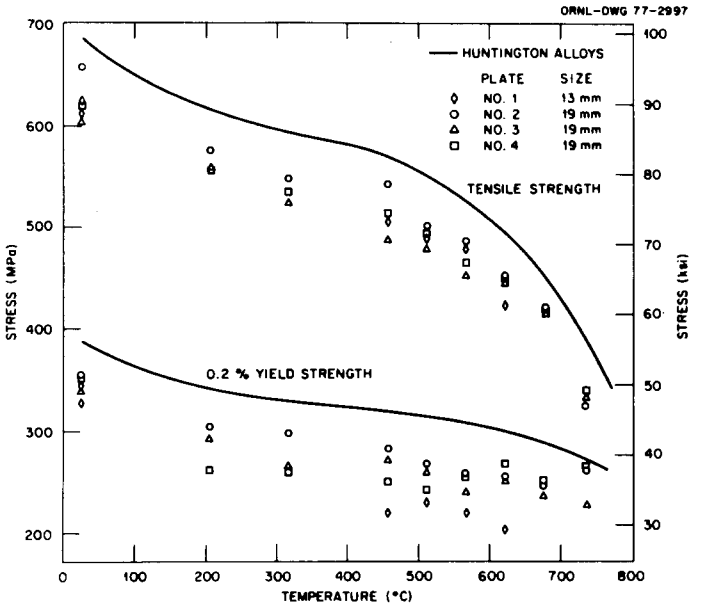

Fig. 1. The 0.2% Yield Strength and Ultimate Tensile Strength as Functions of Temperature for ERNiCr-3 Weld Metal at a Nominal Strain Rate of 3×10^{-4}/s. Four different weldments were tested: Plate 1 was seven-pass weld made on 13-mm-thick plates; Plates 2, 3, and 4 were 40-pass welds made on 19-mm-thick plates. Also shown are curves obtained from Huntington Alloys trade literature.

this conclusion appears premature when the results from plates 3 and 4 are examined (Fig. 1); these two plates were made by the same procedure used to make plate 2.

When the data from all four plates are compared, it appears that plate size has little effect on the ultimate tensile strength over the entire temperature range tested. For the yield strength, on the other hand, there does appear to be a significant difference. The yield strength of the smaller plate falls consistently below that of the welds made on the larger plates (Fig. 1). However, the ultimate tensile strengths for the specimens from both thicknesses were not significantly different. For comparison, the yield strength and ultimate tensile strength curves for ERNiCr-3 taken from manufacturer's literature[1] is also shown in Fig. 1. According to data reported, the referenced material was stronger than the weld metal we tested, although the general trends of the strength with temperature are similar for all the materials.

In general, the ultimate tensile strength data for these tests show a limited amount of scatter, mostly at the lowest test temperatures. At the highest temperatures, the scatter is considerably less. The scatter for the 0.2% yield strength is somewhat greater. If only the data for the welds on the 19-mm-thick plates are considered, the scatter at the highest test temperatures appears considerably less, and the decrease in scatter with increasing temperature is again evident.

The uniform elongation, total elongation, and reduction of area (Fig. 2) for all the tests show considerable scatter, with no real differences evident due to the different weld sizes.

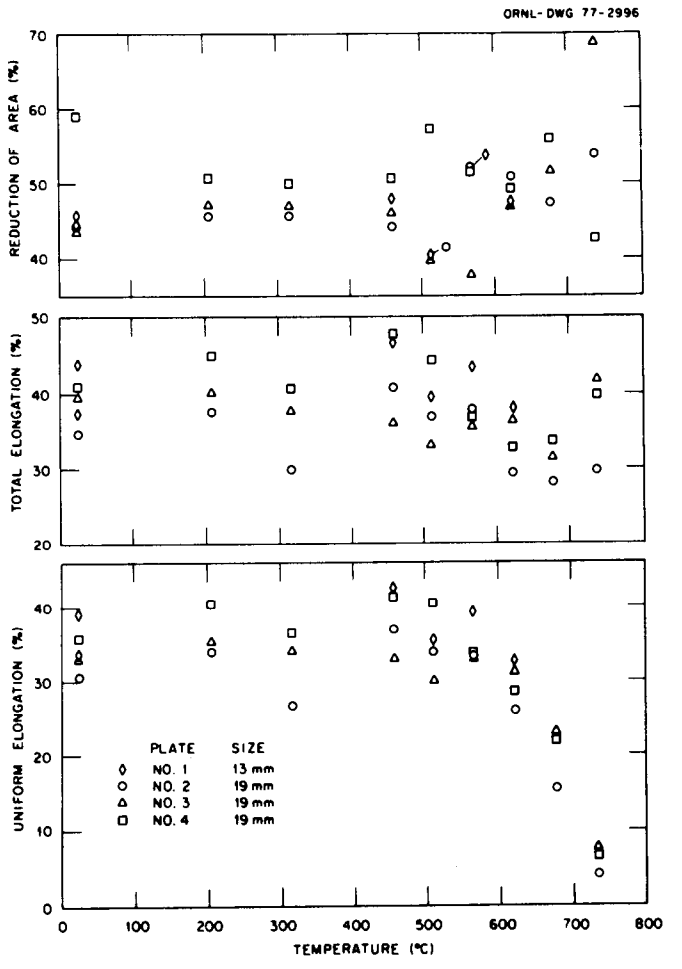

Fig. 2. Uniform Elongation, Total Elongation, and Reduction of Area as Functions of Temperature for the Four Weldments of ERNiCr-3 Tested at 3×10^{-4}/s.

Tests were also made at a nominal strain rate of 3×10^{-6}/s (crosshead speed of 85 nm/s) on specimens taken from plate 3 (Table 3). When the properties are compared with those obtained on the same plate at 3×10^{-4}/s (Fig. 3), one difference is obvious: the low-strain-rate curves for yield strength and ultimate tensile strength as functions of temperature contain marked peaks, which are not as obvious at the higher strain rate. However, closer examination shows apparent similarities in the curves — especially the yield strength behavior. As the temperature is increased from 25°C, the curves for both strain rates first decrease, then remain fairly constant (a strength plateau), and then show a peak. At the low strain rate, the plateau occurs between 200 and 450°C and the peak between 450 and 700°C. For the high strain rate the plateau is between 300 and 450°C and the peak is very much less pronounced. Nevertheless, there does appear to be a slight peak near 621°C. Furthermore, if one examines the data given in Fig. 1 for the other weldments tested at 3×10^{-4}/s, a similar characteristic shape is noted for each curve, and slight peaks can be seen in the data. Obviously, considering the scatter inherent in these data, little can be said about these peaks at the high strain rate.

Table 3. Tensile Properties of ERNiCr-3 Plate 3 Weld Metal[a] at Strain Rate[b] of 3.0×10^{-6}/s

Test Temperature		Strength, MPa (ksi)			Elongation, %		Reduction of Area (%)
(°C)	(°F)	Yield	Ultimate	Fracture	Uniform	Total	
25	75	323(46.9)	598(86.8)	508(73.8)	34.8	39.4	45.5
204	400	256(37.2)	521(75.6)	400(58.1)	34.5	38.6	48.0
316	600	269(39.1)	530(76.9)	425(61.7)	38.6	41.8	50.0
454	850	274(39.7)	511(74.2)	331(48.0)	35.3	39.9	55.2
510	950	329(47.8)	517(75.1)	367(53.3)	30.1	34.9	59.8
566	1050	341(49.5)	482(70.0)	175(25.4)	18.0	25.2	38.1
677	1250	301(43.7)	302(43.9)		0.86	33.8	41.8
732	1350	204(29.6)	206(29.9)	79(11.4)	0.38	39.3	50.5

[a]All specimens were postweld heat-treated for 1 hr at 732°C.

[b]Tests were at a constant crosshead speed of 85 nm/s.

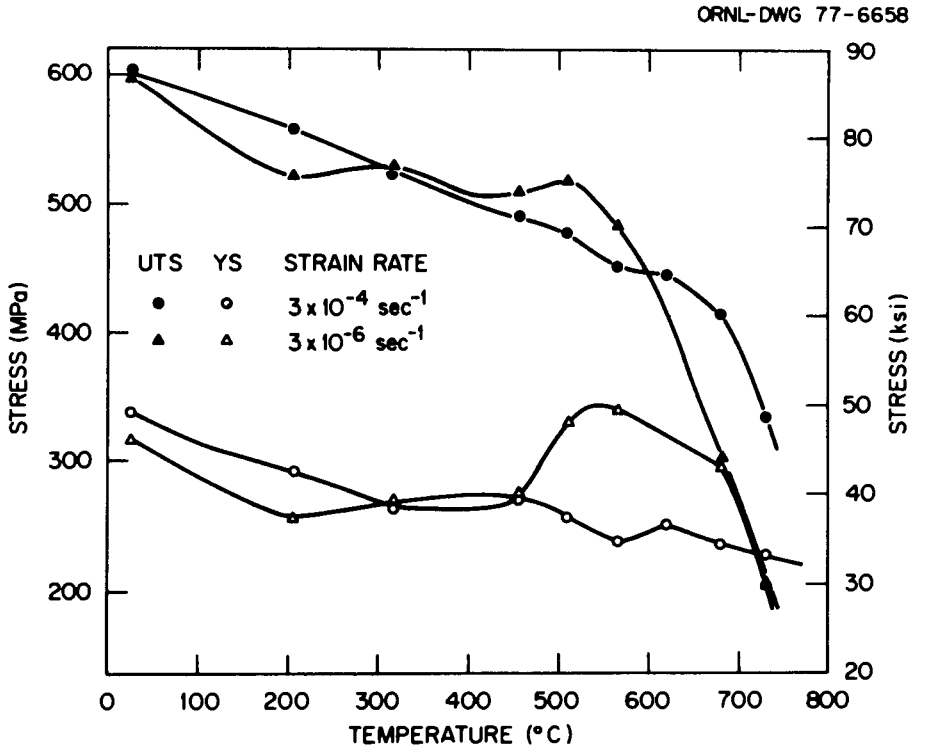

Fig. 3. The 0.2% Yield Strength and Ultimate Tensile Strength as Functions of Temperature for Plate 3 at Nominal Strain Rates of 3×10^{-6} and 3×10^{-4}/s.

For the low-strain-rate data, the relative magnitude of the yield strength peak that occurs above 454°C is greater and occurs at a higher temperature than the ultimate tensile strength peak (Fig. 3). The ultimate tensile strength relationship for the high strain rate shows only the hint of a plateau between 566 and 621°C — the region of the peak in the yield strength curve (Fig. 3). Once the peak in the ultimate tensile strength curve for the low strain rate is reached, the strength rapidly decreases. At 677 and 732°C the yield strength and the ultimate tensile strength differ very little.

The uniform elongation, total elongation, and reduction of area also show no strain rate effects below 454°C. Above that temperature, the most dramatic effect of strain rate occurs in the uniform elongation, which drops off dramatically with increasing temperature (it is only 0.86% at 677°C and 0.38% at 732°C). Total elongation and reduction of area differ only slightly at the two strain rates (Table 3).

To provide an idea of the magnitude of the flow stress peak at strains of interest for design, the stresses for strains of 0.5, 1.0, 2.0 and 5% are given as functions of temperature (Fig. 4). At 3×10^{-4}/s [Fig. 4(b)], the curves have the general characteristics described above for the yield strength. This is most evident at 0.5% strain, where slight peaks occur at 454 and 621°C, with quite a decided minimum in between. This minimum is evident at each strain (and the yield strength curve in Fig. 3), but the "peak" at 454°C becomes quite diffuse.

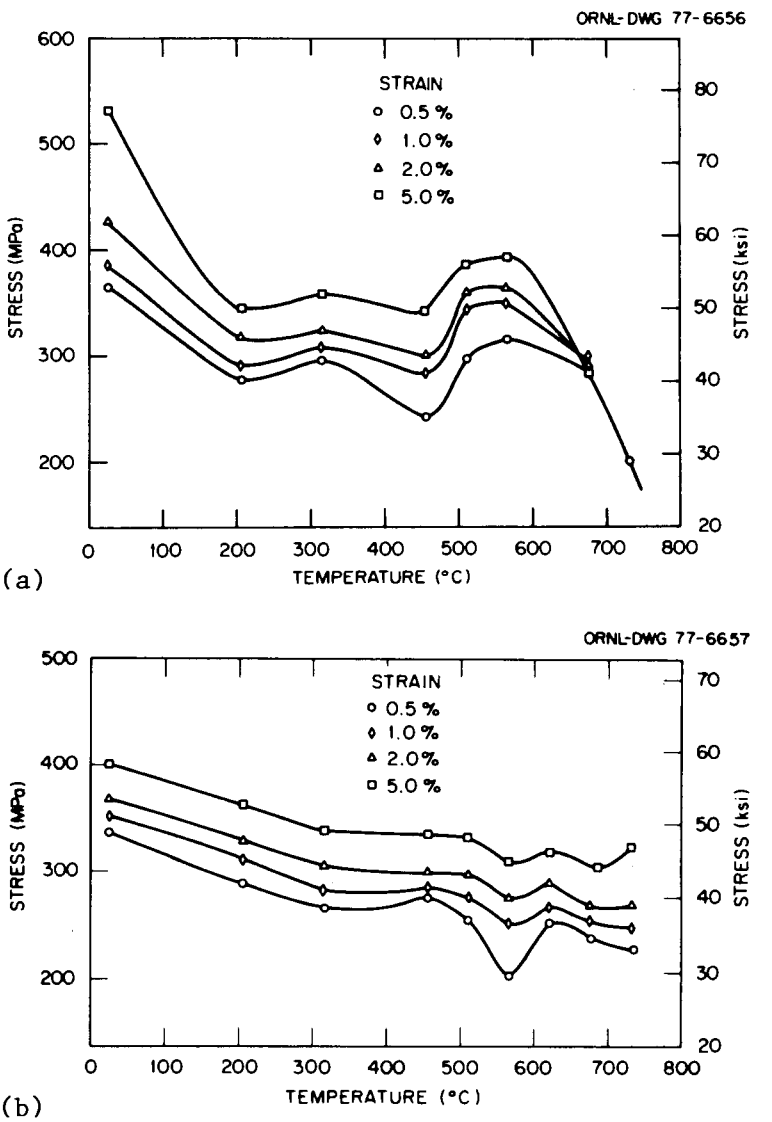

Fig. 4. Flow Stress at Strains of 0.5, 1.0, 2.0, and 5% Strain as a Function of Temperature at (a) 3×10^{-6}/s and (b) 3×10^{-4}/s.

An examination of the individual load-strain curves indicated that jerky flow or serrated yielding occurred. Types A, B, and C serrations, as described by Brindley and Worthington[3] for fcc alloys, were observed (Fig. 5 illustrates the three types, as found by Fahr[4] in type 316 stainless steel). We attempted to characterize the serrations observed on the tests on plate 3 in terms of the stress at which serrations began and their type (Table 4). The largest amplitudes were observed for the low-strain-rate tests.

Brindley and Worthington[3] described these three types of serrations in fcc substitutional alloys as follows:

> Type-A serrations rise above the general level of the stress-strain curve and are periodic in nature. Type-B serrations oscilliate about the general level of the stress-strain curve and occur in rapid sucession. Type-C serrations fall below the general level of the stress-strain curve. All of these different serrations can be made to appear in certain alloys by suitable choice of temperature, strain rate, composition, and grain size.

The different types of serrations are attributed to various types of inhomogeneous deformation:[3]

> Type-A serrations correspond to the propagation of deformation bands along the specimen; Type-B serrations correspond to the formation of parallel band markings formed at random along the gage length; Type-C serrations correspond to the formation of parallel band markings formed at random along the gage length; Type-C serrations correspond to intense local shear bands in some cases.

ORNL-DWG 72-33

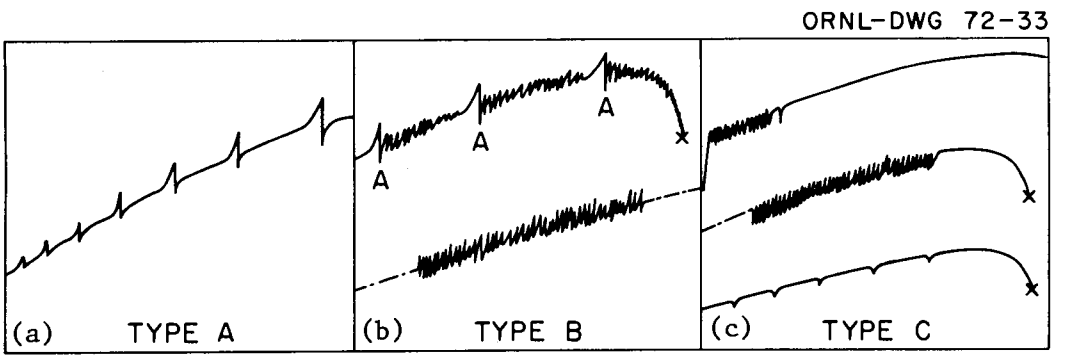

Fig. 5. Types of Serrated Curves as Shown by Fahr (ORNL/TM-4299). (a) Type A. (b) Type B alone (bottom) and Type A combined with Type B (top). (c) Type C.

Table 4. Characterization of Serrated Yielding Behavior of ERNiCr-3 Weld Metal

Test Temperature (°C)	Approximate Strain at Start of Serrations and Serration Type			
	3×10^{-6}/s		3×10^{-4}/s	
	Strain, %	Type	Strain, %	Type
25		None		None
204		None		None
316	1.1	B	0.4	A
454	2.1[a]	C	0.2	B
510	6.7	C	0.6	C
566	2.2	C	1.1	C
621			2.5[b]	C
677		None	1.8	C
732		None	0.9	C

[a]Once serrations begin they are intermittent and have a high amplitude but a low frequency.

[b]Serrations intermittent.

Serrated stress-strain curves are associated with dynamic strain aging.[5] Often alloys that display such behavior also exhibit yield point phenomena — static strain aging. For these tests no such effects were noted. The nearest thing to a yield point was in the 3×10^{-4}/s test at 454°C. At the end of the elastic portion, the curve breaks sharply from the modulus line. Although there is no upper yield point, the curve resembles a curve with a yield point jog (i.e., the Luders extension).

Microstructure

When the etched ERNiCr-3 weld metal microstructure is examined metallographically, a typical weld metal or cast structure is observed (Fig. 6). Although very difficult to resolve, the matrix may contain a widely scattered very fine precipitate. Likewise, any grain boundary

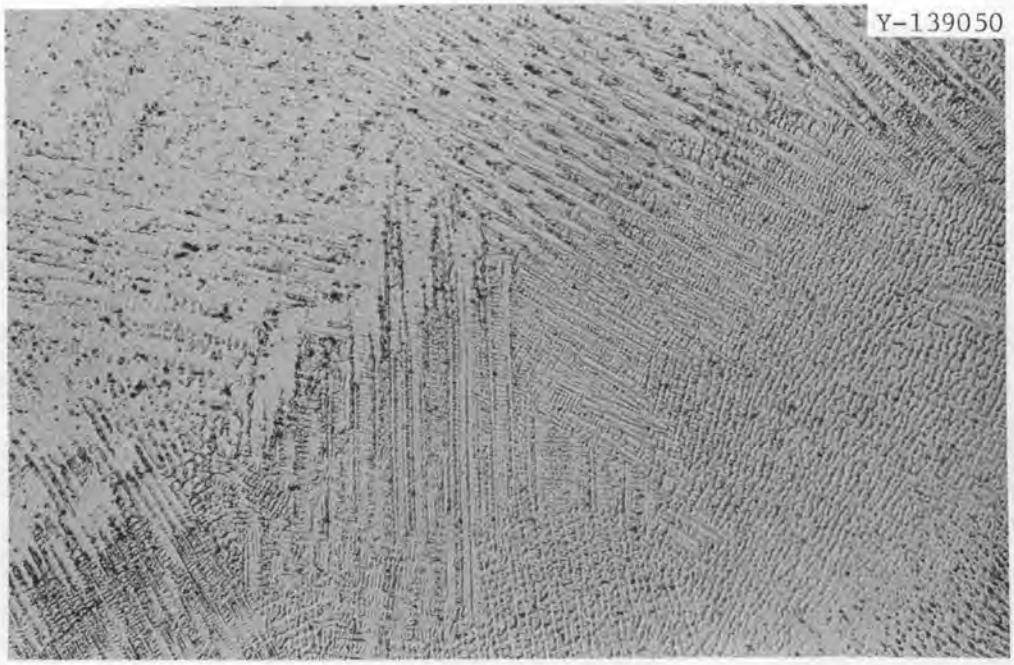

Fig. 6. Microstructure of Undeformed ERNiCr-3 Weld Metal. Etched with 5/1 $HCl-HNO_3$. 100×.

precipitate appears to be quite fine and widely distributed. In general, sound weld metal is observed, which agrees with nondestructive tests, in which no defects could be detected.

In several of the specimens, very small defects were observed metallographically (Fig. 7). These were scattered through the microstructure and too small to be detected by radiography. Those shown in Fig. 7(a) and (b) are larger than most of those observed and can easily be seen as cracks or cavities (voids). Indeed, when the specimen was examined before etching, the nature of these defects could be seen. Also, Fig. 7(b) shows what appear to be some very small cracks or voids on grain boundaries (arrows), although it is impossible to say for certain that they are not precipitate particles. Invariably these defects appear along grain boundaries, and since the large defects are cavities and very little precipitate is noted on grain boundaries, we concluded that these small defects are cavities. This conclusion is enhanced by the small defects shown in Fig. 7(c),

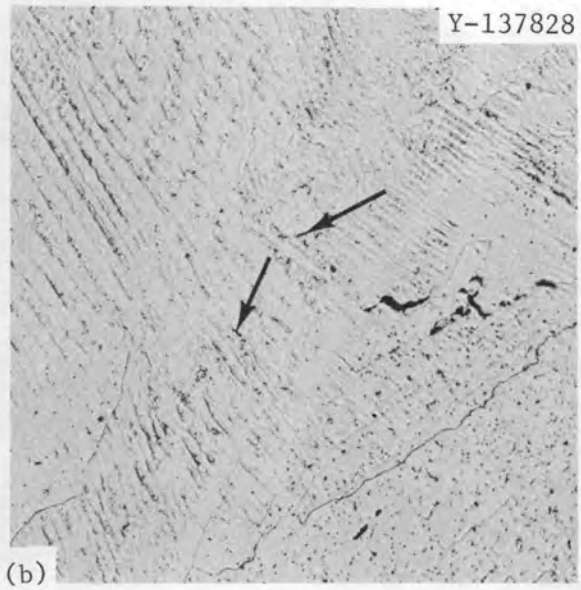

Fig. 7. Examples of Cracks or Voids that were Formed at Scattered Positions in the Weld Metal. Etched with 5/1 $HCl-HNO_3$. (a) 100×. (b) 100×. (c) 200×.

which is at a higher magnification. The size of these defects falls between the large ones and the small ones, and these are easily seen to be cracks or cavities. Also, some small defects of the type are seen in Fig. 7(b), and these now appear as cavities. It should be pointed out that these defects were isolated in only a very small percentage of grain boundaries of a given specimen. Also, in very rare instances, small shrinkage pores were observed. They were quite different from those discussed above and generally appeared in the matrix, not in a grain boundary.

The first two plates tested indicated an effect of weldment size on tensile properties (the specimens from the welds on the 19-mm-thick plates were stronger than those from the 13-mm-thick plates). This would seem to indicate a dilution effect, so we determined the chemical compositions of these two welds and examined them by electron microprobe. The first microprobe studies were qualitative, designed to determine the difference between the concentrations at the edge and center of the weld. Three positions of the weld cross section were examined: the edge near the 2 1/4 Cr-1 Mo steel, midway between edge and center, and at the center of the cross section (Fig. 8 shows the dimensions of the cross sections of the two welds). For both specimens, there was an increased level of iron in the first 20 to 50 mm (iron was the only element that showed any significant variation). The other two positions showed very little difference in iron content. However, the relative peak height for the iron in these two positions was considerably higher for the small specimen than for the large one.

Samples for chemical analysis were taken as shown in Fig. 8. Half a large specimen was sectioned into three pieces, while the entire small specimen was cut into two pieces. The chemical analysis results (Fig. 8) correspond to the qualitative microprobe results in that iron is the only element that varies significantly across the cross section, and it is the only element that deviates from the specifications for this alloy (Fig. 8). The small weld did not allow for a determination of the variability with weld position. Here the

ORNL-DWG 77-2995

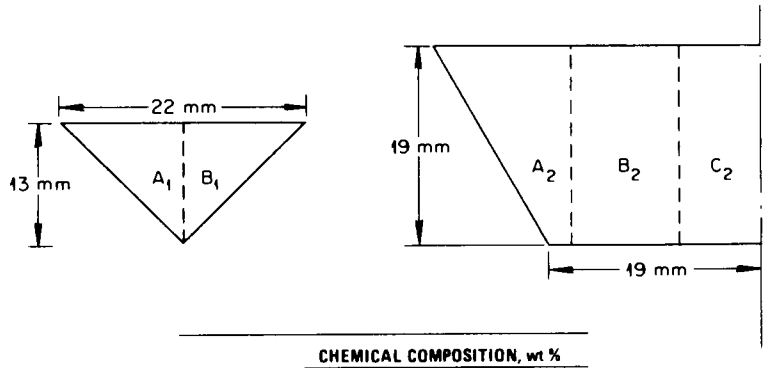

SPECIMEN	CHEMICAL COMPOSITION, wt %				
	Cr	Fe	Mn	Nb	Ti
A_1	18	10	2.7	1.7	0.3
B_1	18	10	2.7	1.9	0.3
A_2	18	4.1	2.9	2.8	0.3
B_2	17	1.9	3.0	2.4	0.3
C_2	18	1.7	2.9	2.2	0.3
SPECIFICATION					
min	18.0		2.5	2.0	
max	22.0	3.0	3.5	3.0	0.75

Balance is Ni

Fig. 8. Cross-Sectional Dimensions for the Small and Large Welds and the Chemical Compositions Determined in Various Parts of the Welds.

iron content was 10 wt % throughout the sample. The chemical specifications for ERNiCr-3 weld rods allow a 3% maximum. Thus, there appears to be a significant dilution throughout the cross section during welding. On the other hand, results for the large weldment indicate that the dilution is restricted to the vicinity of the fusion line.

To determine the concentration gradient profile for iron in the large specimen, half of the specimen was probed with a static spot x-ray step scan every 1.25 mm from the edge to the specimen center (Fig. 9). The elevation of the scan was in the upper half of the cross section. Standardized on the concentration of 1.7 wt % Fe at the specimen center as determined by chemical analysis, the concentration dropped rather quickly in the first 1.25 mm from 8% at the specimen edge to about 2%, after which it remained constant out to about 7.5 mm. At that position, the concentration dropped to 1.7% — the standardized composition. This latter drop appeared to coincide with the change from one weld pass to another.

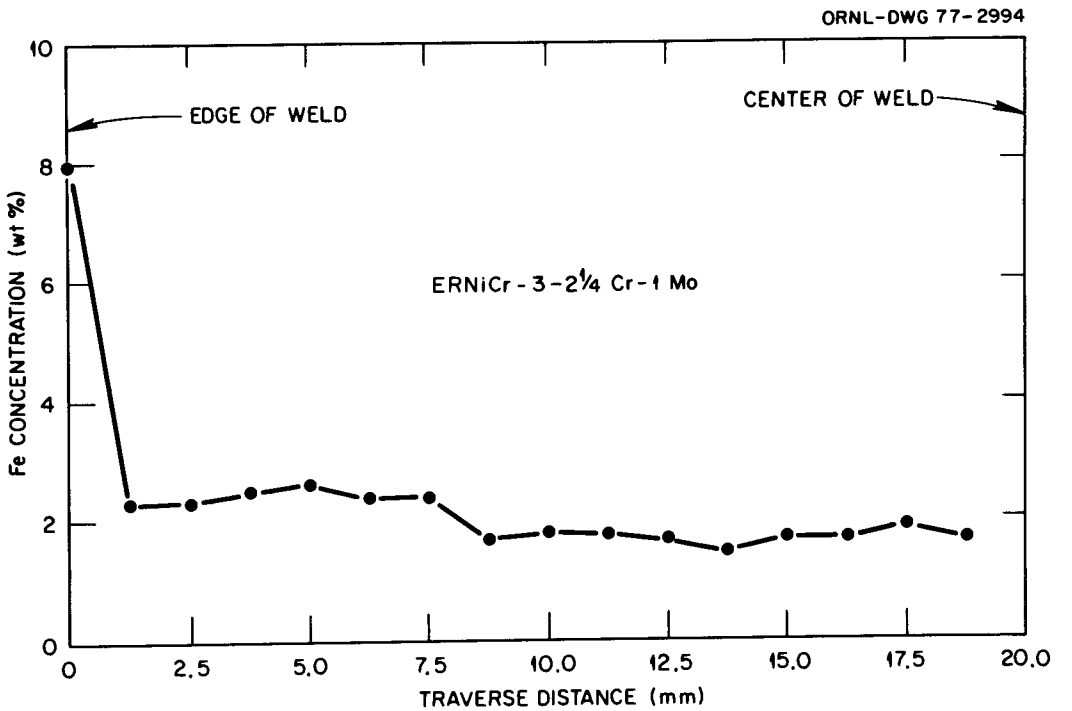

Fig. 9. Iron Cencentration Profile from the Edge to the Center of a Large Weld.

When inspected visually, the deformed specimens displayed evidence of anisotropic deformation. The specimen surfaces were fibrous or rumpled parallel to the specimen axis. In many cases the specimens also had a "knobby" appearance. That is, usually one or more points on the specimen gage section, in addition to the region that necked to failure, appeared to be in the process of neck formation. All specimens necked, but most deformed to an elliptical rather than circular cross section. The failures of the specimens tested at 3×10^{-4}/s up to 510°C appeared to be of a shear type. At the higher temperatures, a cup-cone fracture occurred. All the failures at the low strain rate (3×10^{-6}/s) were the shear type. The fracture surfaces of the low-strain-rate tests at 566 and 677°C appeared to contain two differently colored regions — one darker than the other — an indication that the specimens may have partially fractured and oxidized before the fracture was complete.

Selected fractured specimens were sectioned and examined metallographically. All the failures appeared to be transgranular and

were accompanied by considerable distortion of the grains near the fracture. However, on numerous specimens, isolated cracks appeared in the gage section (Figs. 10 to 12). Invariably, when examined on etched specimens, these cracks were found in grain boundaries. The photomicrographs in Fig. 10 are from a specimen that failed near the end of the gage section where the extensometer was attached (it had a reduced ultimate tensile strength and ductility). This specimen had considerably more cracks than any of the others; indeed, the appearance of the fracture surface indicates that the failure had considerable intergranular character. Although the number of cracks and mode of failure for this specimen are atypical, the photomicrographs display the type of cracks that were observed in much smaller number on other specimens. On other specimens (Figs. 11 and 12), not as many instances of grain boundary separation were noted. Except in the specimen that failed at the end of the gage section, the number of grain boundary cracks per specimen were few and scattered through the cross section and did not appear to affect the fracture. The number of cracks per specimen appeared to increase with increasing temperature and decreasing strain rate.

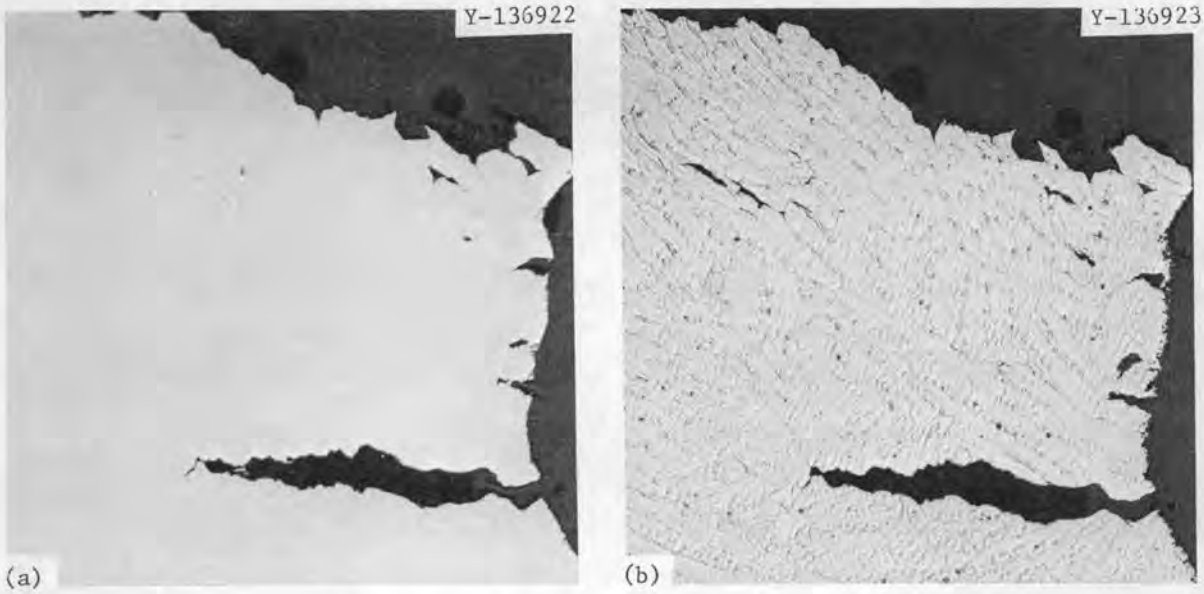

Fig. 10. Example of Cracks on a Specimen Tested at 677°C and 3×10^{-4}/s. The specimen failed prematurely. 100×. Reduced 13%. (a) As polished. (b) etched with 5/1 HCl-HNO_3.

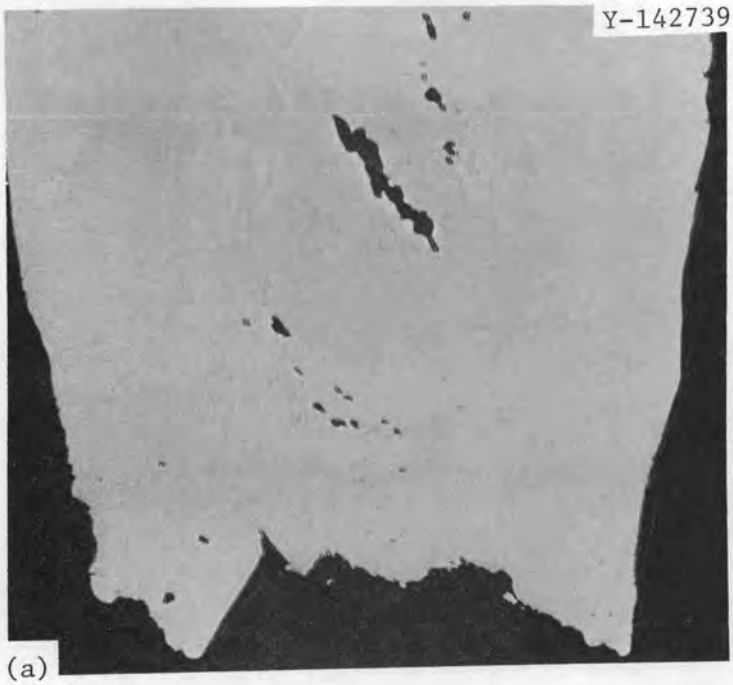

(a)

(b)

Fig. 11. Example of Cracks on Specimen Tested at 732°C and 3×10^{-4}/s. (a) As polished. 50×. (b) Etched with 5/1 HCl-HNO . 200×.

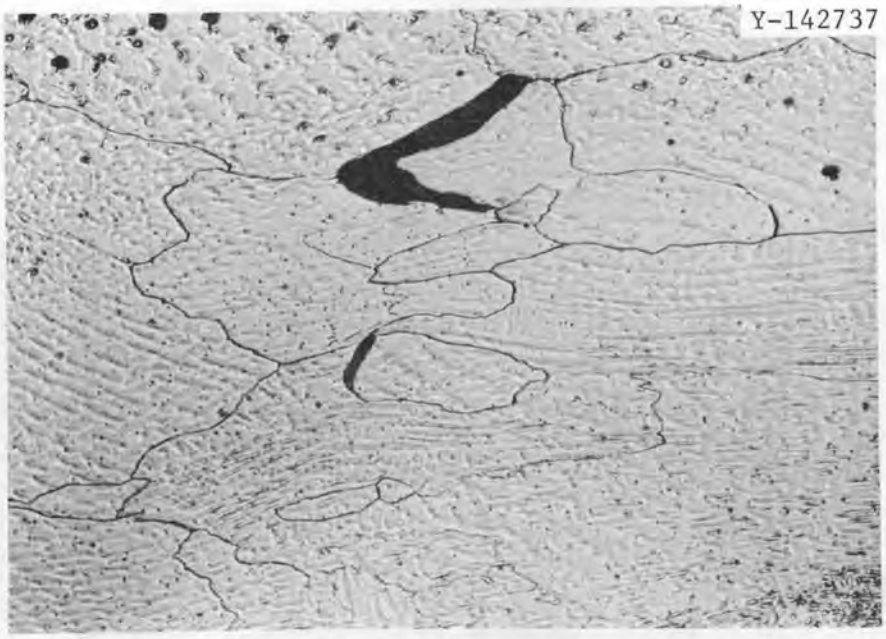

Fig. 12. Example of Grain Boundary Cracks in Specimen Tested at 677°C and 3×10^{-4}/s. Etched with 5/1 $HCl-HNO_3$. 200×.

The anisotropic deformation that caused the "knobby" deformation was a result of the weld metal microstructure (Fig. 13). Figure 13(a) shows that the "knob" in this case occurred near the intersection of several grains. In Fig. 13(b) the anisotropic deformation was the result of grain boundary cracks in material adjacent to the external surface.

DISCUSSION

Although the analytical chemistry and microprobe results indicate a significantly greater dilution of the weld metal by iron in the welds made on the 13-mm-thick plate than the 19-mm-thick plate, the only effect on tensile properties appears to be on the yield strength at elevated temperatures. Thus, the decisive difference in Fig. 1 is not the difference between the weld metal from the different geometries, but the difference between the strength of the weld metal from this study and commercial literature or Payne's data.[1,2]

Since the commercial manufacturer made its welds on alloy plates with chemical composition similar to the ERNiCr-3 weld metal,[6] the

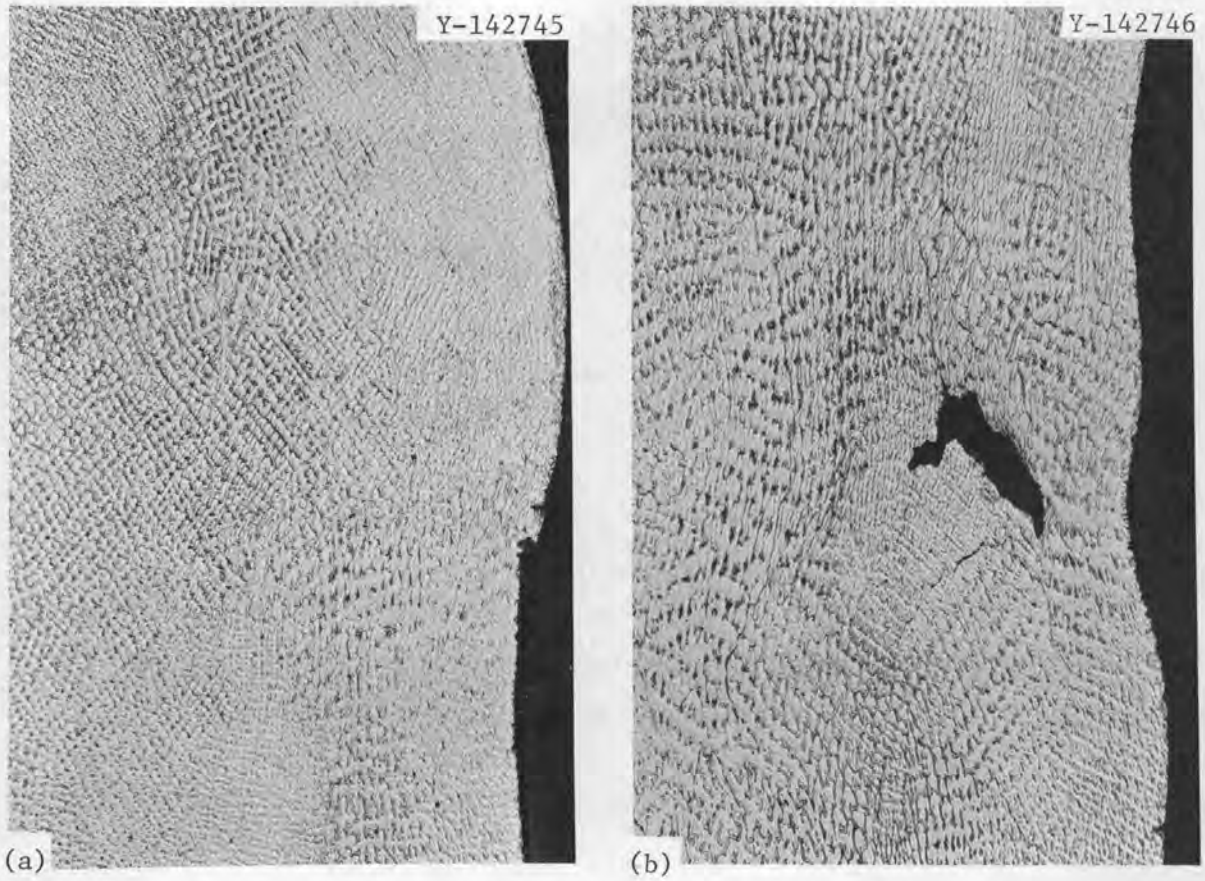

Fig. 13. Photomicrographs that Demonstrate the Reasons for Knobby Deformation. Knob forms (a) adjacent to position where several grains meet and (b) adjacent to grain boundary cracks. Etched with 5/1 $HCl-HNO_3$. 100×.

dilution of their welds was probably considerably less than the obtained in the present study (no information was available on how Payne's welds were made). As seen above, however, dilution produces a quite minor effect on the ultimate tensile strength. The commercial manufacturer and Payne[2] give no information on postweld heat treatment, indicating that their properties are for as-deposited ERNiCr-3 weld metal. Presumably, this latter effect is the major cause of the strength differences. Furthermore, Payne[2] states that, "Dilution of nickel welding products with copper will reduce the mechanical properties, but iron and chromium dilution will increase them."

As stated in the RESULTS section, the incidence of grain boundary cracking increased slightly with increasing temperature and decreasing

strain rate. However, with the exception of the specimen that failed near the end of the gage section, these cracks were relatively few and isolated throughout the cross section. In other words, we noted no specific indication of a change in fracture mode from transgranular to intergranular. Although no direct correlation is possible, the observations of isolated grain boundary "defects" in the as-welded material coupled with the observations of grain boundary cracks in the failed tensile specimens are probably related. This conclusion is buttressed by the observation that often when several grain boundary cracks were observed on a metallographic surface, they were confined to one region of the specimen, usually a single pass. A similar observation was made on the grain boundary defects in as-welded material. Further study is required before the nature of these defects can be identified.

Serrated yielding or jerkey flow can be explained in terms of dynamic strain aging effects[3,5,7] (i.e., in terms of interactions between dislocations and solutes in the alloy). The effect occurs under conditions where the solute can diffuse rapidly enough to slow down a moving dislocation by forming a solute atmosphere. In fcc alloys, serrated yielding is most often explained in terms of interactions with substitutional atoms, although evidence exists that such effects can also arise from interactions between interstitial solutes and dislocations. Serrated yielding over certain ranges of temperature for stainless steels[4,8] is attributed to the interaction of carbon-vacancy pairs with dislocations. Evidence also exists for interstitial-dislocation interaction to account for serrated yielding in the niobium-carbon[9,10] and niobium-hydrogen[11,12] systems and in nickel austenitics that contain carbon.[13]

Because of its high diffusion rate, carbon-associated serrated yielding is generally restricted to temperatures lower than those observed in the present investigation. Serrations caused by carbon in nickel[9,10] and high-nickel austenitics[13] occur below 300°C. Effects attributed to carbon in stainless steels[8] occur below 500°C. In the present investigation, serrations became most pronounced above 500°C. Although these observations cannot be used to rule out carbon as

the cause of some of the observations, substitutional solutes apparently must be playing a role. Detailed study could determine the cause of these serrations. However, that is beyond our present scope.

One of our most interesting observations was the increase in flow stress at low strain rates between 500 and 650°C (Figs. 3 and 4). In bcc materials, dynamic strain aging due to carbon or nitrogen can lead to such effects.[7] Peaks attributable to carbon have also been observed in fcc alloys such as nickel[10] and stainless steel.[8] In nickel the peaks formed below 300°C; those in stainless steel formed below 500°C and were rather insensitive to strain rate (also, such effects usually show up on the ultimate tensile strength rather than yield strength).

It appears, therefore, that the increase in flow stress noted above 454°C is not due to interstitials. However, the plateau or slight peak noted at lower temperatures could be due to interstitials, although more work would be required to verify this.

As pointed out above, serrated yielding in fcc alloys can result from interactions between dislocations and substitutional solute atoms. However, such interactions do not lead to effects on flow stress.[3,5] Hence, some other process must cause the observed effect.

Anomalous behavior with temperature in the physical and mechanical properties of nickel-chromium alloys has been studies by many investigators[14–17] (most studies have been on Ni–20% Cr, which is used extensively as electrical resistance and thermocouple material). In most of these studies, electrical resistivity changes have been investigated as a function of temperature. Instead of the expected continuous increase in resistivity with temperature, the resistivity generally increases to about 450 or 500°C. Between about 500 and 700 to 800°C, the resistivity goes through a local minimum. Along with the changes in resistivity, changes have also been noted in room-temperature hardness,[17] lattice spacing,[16] and specific heat.[16,17]

Over the years several explanations have been advanced for this behavior. Most often the explanations involve short-range order,[14,16,18] electron transfer to shells of atoms of the tranistion elements in the alloy[15,19]

or the clustering of atoms of one of the alloy components.[17] Others have proposed that both ordering and electron-transfer occur.[16,20] Thomas[15] attributed the effect to a structural state of the material that he called the "K-state." He found that the K-state also formed in Fe-Al, Fe-Si, Ni-Al, Ni-Cu, and Ni-Cu-Zn. According to Thomas, the only necessary condition for K-state formation is that the alloy contain at least one transition element — that is, an element with an incomplete inner electron shell.

McCoy and McElroy[21] studied the resistivity behavior of eight commercial nickel-base alloys that contained Fe, Cr, and Mo from 25 to 1000°C. All these alloys displayed the behavior typified by a K-state. They proposed that short-range order caused the effect. Recently, Williams[22] noted a similar resistivity behavior for the ERNiCr-3 weld metal of the type studied in the present investigation. He found that the resistivity begins to decrease near 500°C and decreases up to 700°C. Hence, indications are that the observations on the effect of strain rate on flow stress between 450 to 650°C in ERNiCr-3 weld metal (Figs. 3 and 4) are due to the K-state.

To determine order in an alloy, the most direct technique is by x-ray diffraction. However, because of the similarity of the x-ray atomic scattering factors for nickel and chromium, the interpretation becomes extremely difficult for nickel-chromium alloys. Neutron diffraction, for which nickel and chromium have considerably different atomic scattering factors, should be the best technique for studying order in these alloys. Roberts and Swalin[23] found no ordering in a neutron diffraction study on a Ni—25 at. % Cr alloy. However, x-ray studies by Baer[24] showed that an ordered phase identified as Ni_2Cr exists between 25 and 36 at. % Cr. This was confirmed by other investigators.[25—27] As a result, an order-disorder phase boundary is "dotted" into the phase diagram given by Shrunk.[28] According to this diagram and the previous one given by Hansen[29] (the phase field in Hansen's diagram was accompanied by a question mark), the upper temperature of the order-disorder reaction is at about 550°C.

Very few studies have dealt with the effect of the K-state on mechanical properties. Clayton and Brooks[30] studied the room

temperature tensile properties of nickel alloys containing 10, 20 and 30% Cr that were given different heat treatments. They showed that the alloys slowly cooled from 900°C or isothermally annealed at 530°C were stronger than those quenched from 900°C. The results were taken by Clayton and Brooks to be "suggestive of an increase in the amount of short range order," since "the short annealing times preclude long range order occurring."[30] The greatest effect occurred for the 30% Cr alloy, which would be expected in light of the phase diagram.[28]

The formation of both short-and long-range order is expected to lead to changes in the strength of an alloy.[31,32] Fisher,[33] who first discussed the effect of short-range order on strength, stated that as a dislocation passes through an ordered lattice, order bonds are destroyed. This requires the formation of an interface, which will require energy above that required by a dislocation moving through the unordered lattice. Once the order on the slip plane has been reduced by the first dislocation, subsequent dislocations can move through the slip plane at a reduced stress, and the stress to move a series of dislocations along a slip plane should drop progressively.

The effect of order on mechanical properties is usually studied in terms of the effects on flow stress or yield point. Specimens are aged for various times at a temperature at which order occurs and are then tensile tested at room temperature.[30,34,35] Short-range order occurs above T_c, the critical temperature at which long-range order begins to form. As the amount of order increases with a decrease in temperature or prolonged annealing in the ordering temperature range, it becomes more difficult to move a single dislocation through the ordered alloy because of the Fisher[33] mechanism. Eventually it is impossible to move a single dislocation through the superlattice, because of the large amount of energy required for the dislocation to disrupt more and more order relationships.[34,35] At that point deformation occurs by the movement of super dislocations, which consist of paired dislocations connected by antiphase boundary. As the first dislocation moves through the lattice, it destroys order bonds. The second dislocation, however, restores the order bonds. Since the

movement of super dislocations leaves the order relationships unchanged, the stress required for deformation will fall.

Room-temperature tensile tests on alloys quenched from various temperatures or tensile tests at temperature show that the flow stress goes through a maximum when plotted against annealing or test temperature.[30,32,34,35] A plot of the data against the long-range order parameter, S, inevitably shows that the flow stress maximum occurs for a partially ordered alloy. Besag and Smallman[34] showed that the maximum occurs near the point where deformation changes from being controlled by single dislocations to super dislocations.

The interpretation of the effect of strain rate on flow stress shown in Figs. 3 and 4 can tentatively be explained in terms of nickel-chromium observations on short-range order or K-state. Of course, ERNiCr-3 weld metal is somewhat more complicated than the binary nickel-chromium alloy. However, nickel and chromium are the major constituents and their ratio approaches that in which Clayton and Brooks[30] noted their largest effect (it also approaches the Ni_2Cr composition[28]).

If we accept the proposal that the K-state in nickel-chromium is due to order,[24—27] then we can tentatively conclude that a similar process occurs in ERNiCr-3. We further conclude that the effects are due to short-range order, since the alloy was not annealed for sufficient times at the ordering temperatures to induce long-range order.[24,31]

To try and visualize a possible explanation for the strain rate effects, consider Fig. 14, which shows the first 5% of the stress-strain curves at 510 and 566°C at the two different strain rates. Although flow stress differs considerably (Fig. 4), the work-hardening rate at the two different strain rates is essentially the same. One possible explanation for these observations is that above 500°C, diffusion is rapid enough to form regions of short-range order during the test. Hence, order should form while the specimen is being heated to the test temperature; also, some order might already be present, having formed when the specimens cooled after tempering.

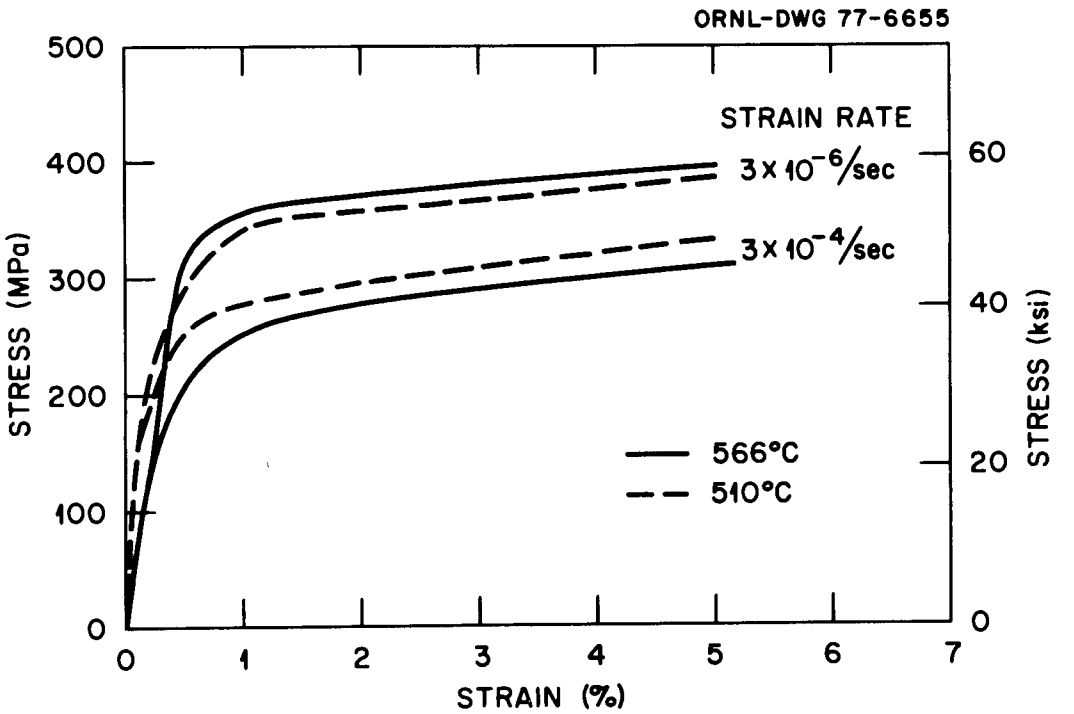

Fig. 14. Stress-Strain Curves for ERNiCr-3 at Strain Rates of 3×10^{-6}/s and 3×10^{-4}/s and 510 and 566°C.

In accordance with the Fisher mechanism,[33] for the high-strain-rate (3×10^{-4}/s) tests, the first dislocation that moves through the lattice destroys the short-range order relationship. Subsequent dislocations will not have to destroy that order and will move more easily across that same slip plane. On the other hand, at the low strain rate (3×10^{-6}/s), the velocity of the dislocations through the lattice is considerably reduced. Hence, if diffusion is rapid enough, the destroyed order bonds will be healed before subsequent dislocations pass. Thus, each dislocation will have to break order bonds (destroy regions of short-range order).

The work-hardening rate is generally thought to depend on the interaction of moving dislocations with other dislocations that cross the slip plane. Since the work-hardening rates for the two strain rates are similar (Fig. 14), we would conclude that the difference in the flow stress is simply the extra stress required to move the dislocations through the lattice at the two different strain rates.

In the one case the dislocations move continuously through regions of short-range order, while in the other the dislocations move through a disordered lattice — after the short-range order has been destroyed by the passage of the initial dislocations.

The flow strength maximum at low strain rates occurs when recovery effects become important. Eventually, the strength at the low strain rates falls below that at the high strain rates because of recovery effects. The observation that the peak was much more pronounced in the yield strength curve can also be explained. Recovery generally affects the ultimate tensile strength more than the yield strength. Furthermore, deformation introduces disorder into the lattice; the amount of disorder introduced increases with deformation.

The yield strength peak at the high strain rate could be explained by the same process. As the test temperature is increased, the rate of diffusion increases; eventually, diffusion rates are rapid enough to repair short-range-order bonds, even as the dislocations are moving at the higher rate. A more subdued peak would be expected, since the degree of short-range order decreases with increasing temperature.

In the future, experiments are planned to further explore these effects. Needless to say, the above results should have implications in creep studies, where strain rates are considerably less than those of this study. We are presently conducting such tests.

SUMMARY AND CONCLUSIONS

Tensile properties were determined for ERNiCr-3 weld metal over the range 25 to 732°C at strain rates of 3×10^{-4} and 3×10^{-6}/s. Tests were made on four gas tungsten-arc weldments: three 40-pass welds with a 32-mm root opening and on one seven-pass weld with 90°-included-angle V-groove joint. The following results and conclusions were obtained:

1. Optical microscopy showed scattered grain boundary defects through the microstructure of the weld metal. These defects appeared to be small cracks or voids that could not be detected by radiography, even when 28.6-mm-diam rods were inspected.

2. The two different weld sizes were examined for base metal dilution effects. The only dilution noted was for iron. Much more dilution was present in the small weld.

3. At the higher strain rate (3×10^{-4}/s), where most of the tests were made, the effect of weldment size had no noticeable effect on the ultimate tensile strength and ductility. However, the yield strength of the specimens from the small weldment fell consistently below those for the large weldment.

4. For temperatures below 454°C, the properties measured for the lower strain-rate tests (3×10^{-6}/s) were similar to those at the higher strain rate. At temperatures above 454°C, both the yield strength and the ultimate tensile strength relationship with temperature had peaks. The yield strength had a maximum between 550 and 600°C and the ultimate tensile strength had a local maximum around 500°C. The yield strength for the low strain rate remained above that for the high strain rate up to the highest test temperature (732°C). The ultimate tensile strength for the low strain rate, however, approached that for the high strain rate at about 600°C, then rapidly decreased and fell below that of the highest strain rate. Although the total elongation and reduction of area were little affected by strain rate, the uniform elongation dropped precipitously with increasing temperature at the lower strain rate, having a value of 0.39% at 732°C.

5. The peaks in the temperature dependences of yield strength and ultimate tensile strength at the lower strain rate were attributed to short-range-order effects. This conclusion is based on work of other investigators, primarily on nickel-chromium alloys. The observed peak in tensile properties corresponds to a similar peak observed in the electrical conductivity of ERNiCr-3.

6. Serrated flow curves were observed. Three types of serrations were identified.

7. All tensile specimens failed by a transgranular mode. However, scattered grain boundary separations were observed on numerous specimens. Although no direct evidence was found to relate these cracks with the grain boundary defects observed on the untested specimens, we suspect that the two are related.

ACKNOWLEDGMENTS

Several people aided in completing this work: J. L. Griffith and L. T. Ratcliff conducted the tests; C. W. Houck carried out the metallography; G. M. Goodwin, R. K. Williams, G. M. Slaughter, and C. R. Brinkman reviewed the manuscript; Sigfred Peterson edited the manuscript; and Gail Golliher prepared the final version.

REFERENCES

1. Huntington Alloys, *Incoloy Alloys*, International Nickel Company, Inc., Huntington, W. Va., 1973.
2. B. E. Payne, "Nickel-Base Welding Consumables for Dissimilar Metal Welding Applications," *Met. Constr. Br. Weld. J.* 1(12s): 79–87 (1969).
3. B. J. Brindley and P. J. Worthington, "Yield Point Phenomena in Substitutional Alloys," *Metall. Rev.* 145, *Met. Mater.*, 4: 101–14 (1970).
4. D. Fahr, *Analysis of Stress-Strain Behavior of Type 316 Stainless Steel*, ORNL/TM-4299 (November 1973).
5. J. D. Baird, "Dynamic Strain Aging," pp. 191–222 in *The Inhomogeneity of Plastic Deformation*, American Society for Metals, Metals Park, Ohio, 1973.
6. S. Keiser, Huntington Alloys, private communications.
7. J. D. Baird, "The Effects of Strain-Aging Due to Interstitial Solutes on the Mechanical Properties of Metals," *Metall. Rev.* 149, *Met. Mater.* 5: 1–18 (1971).
8. C. F. Jenkins and G. V. Smith, "Serrated Plastic Flow in Austenitic Stainless Steel," *Trans. Metall. Soc. AIME* 245: 2149–56 (1969).
9. D. E. Sonon and G. V. Smith, "Effect of Grain Size and Temperature on the Strengthening of Nickel and a Nickel-Cobalt Alloy by Carbon," *Trans. Metall. Soc. AIME* 242: 1527–33 (1968).
10. V. F. Sukharov et al., "Strain-Aging of Nickel," *Fiz. Met. Metalloved.* 14: 895–98 (1962).

11. B. A. Wilcox and G. C. Smith, "The Portevin-Le Chatelier Effect in Hydrogen Charged Nickel," *Acta Metall.* 12: 371–76 (1964).

12. Y. P. Nechay and K. V. Papov, "Effect of Hydrogen on the Temperature Dependence of the Flow Stress of Nickel and Stainless Steel," *Phys. Met. Metalloved.* 21: 109–13 (1966).

13. K.S.B. Rose and S. G. Glover, "A Study of Strain-Aging in Austenite," *Acta Metall.* 14: 1505–16 (1966).

14. Z. Yano, "On the Anomaly in the Nickel-Rich Solid Solution of Nickel-Chromium Binary System," *Rikwagku-Kenkyo-Jo-Iho* 19: 110–17 (1940).

15. H. Thomas, "Uber Widerstandslegierrungen," *Z. Phys.* 129: 219–32 (1951).

16. A. Taylor and K. G. Hinton, "Study of Order-Disorder Precipitation Phenomena in Nickel-Chromium Alloys," *J. Inst. Met.* 81: 169–80 (1952).

17. B. G. Livshitz et al., *Investigations of Heat-Resistant Alloys,* Vol. 2, USSR Academy of Sciences Publishing House, Moscow, 1957.

18. Y. Imai and T. Masumoto, "Anomalous Contraction Near 500°C in Austenitic Heat Resisting Alloys Containing Chromium and Nickel," *Scientific Reports of the Research Institute, Tohoku University,* 14(A): 1–10 (1962).

19. A. Schulz, "Electrical Conductivity of Fe-Cr-Al Alloys Containing Cold Work," *Z. Metallkd.* 42: 120–22 (1951).

20. V. Meskin et al., "Electrical Resistivity Anomalies and the Formation of a K-State in the Systems Pa-W and Pa-Mo," *Phys. Met. Metallog.* 13(1): 113–17 (1962).

21. H. E. McCoy, Jr., and D. L. McElroy, "Electrical Resistivity Anomaly in Nickel-Base Alloys," *ASM Trans. Quart.* 61(4): 730–41 (1968).

22. R. K. Williams, Oak Ridge National Laboratory, private communications.

23. B. W. Roberts and R. A. Swalin, "Concerning an Order-Disorder Transition in the Ni-Cr System," *Trans. Metall. Soc. AIME* 209: 845–46 (1957).

24. H. G. Baer, "Superstructure and K-State in Ni-Cr System," *Z. Metallkd.* 49: 614–22 (1958).

25. N. V. Semenova, "On the Question of the Anomaly in the Electrical Resistance of the Alloy Ni_3Cr," *Phys. Met. Metallog.* 6(b), 57–66 (1958).

26. H. Schuller and P. Schwaab, "Electron Diffraction Investigation of the Sigma-Phase in the Cr-Fe and Cr-Ni Systems," *Z. Metallkd.* 51: 81–4 (1960).

27. R. G. Davies, "An X-Ray and Dilatometric Study of Order and K-State in Iron-Aluminum Alloys," *J. Phys. Chem. Solids* 24: 985–92 (1963).

28. F. A. Shrunk, *Constitution of Binary Alloys, Second Supplement,* McGraw-Hill, New York, 1969.

29. M. Hansen, *Constitution of Binary Alloys,* McGraw-Hill, New York, 1958.

30. W. E. Clayton and C. R. Brooks, "Tensile Mechanical Properties at 25°C of High Purity, Binary Nickel-10, -20, -30 Percent by Weight Chromium Alloys," *J. Mater.* 5: 157–68 (1970).

31. R. W. Cahn, "Correlation of Local Order with Mechanical Properties," pp. 179–214 in *Local Atomic Arrangements Studied by X-Ray Diffraction,* eds. J. B. Cohen and J. E. Hilliard, AIME, New York, 1965.

32. N. S. Stoloff and R. G. Davies, "The Mechanical Properties of Ordered Alloys," *Progress in Materials Science* 13(1), Pergamon Press, New York, 1966.

33. J. C. Fisher, "On the Strength of Solid Solution Alloys," *Acta Metall.* 2: 9–10 (1954).

34. F.M.C. Besag and R. E. Smallman, "Changes in Yield Behavior and Microstructure in Ni_3Fe and Ni_3Mn Upon Ordering," pp. 259–74 in *Ordered Alloys: Structural Applications and Physical Metallurgy,* eds. B. H. Kera et al., Claitor's Publishing Division, Baton Rouge, Louisiana, 1970.

35. N. S. Stoloff and R. G. Davies, "The Plastic Deformation of Ordered FeCo and Fe_3Al Alloys," *Acta Metall.* 12: 473–85 (1964).

ORNL-5354
Distribution
Category
UC-79b, -h, -k

INTERNAL DISTRIBUTION

1–3. Central Research Library
4. Document Reference Section
5–14. Laboratory Records Department
15. Laboratory Records, ORNL RC
16. ORNL Patent Office
17. G. M. Adamson, Jr.
18. S. E. Beall
19. R. G. Berggren
20. M. K. Booker
21. C. R. Brinkman
22. D. A. Canonico
23. J. A. Conlin
24. J. M. Corum
25. J. E. Cunningham
26. J. H. DeVan
27. J. R. DiStefano
28. R. G. Donnelly
29. D. P. Edmonds
30. W. R. Gall
31. G. M. Goodwin
32. R. J. Gray
33. W. L. Greenstreet
34. W. O. Harms
35. T. L. Hebble
36. R. F. Hibbs
37–39. M. R. Hill
40. J. P. Hammond
41. D. O. Hobson
42. J. A. Horak
43. H. Inouye
44. P. R. Kasten
45–48. J. F. King
49. R. T. King
50–54. R. L. Klueh
55. J. M. Leitnaker
56. A. L. Lotts
57. C. T. Liu
58. K. C. Liu
59. R. E. MacPherson
60. W. R. Martin (Y-12)
61. H. E. McCoy, Jr.
62. H. C. McCurdy
63. C. J. McHargue
64. A. J. Moorhead
65. R. K. Nanstad
66. H. Postma
67. P. Patriarca
68. C. E. Pugh
69. J. L. Scott
70. V. K. Sikka
71. G. M. Slaughter
72. W. J. Stelzman
73. J. O. Stiegler
74. J. P. Strizak
75. R. W. Swindeman
76. D. B. Trauger
77. W. E. Unger
78. J. R. Weir, Jr.
79. G. D. Whitman
80. R. W. Balluffi (consultant)
81. P. M. Brister (consultant)
82. W. R. Hibbard, Jr. (consultan
83. N. E. Promisel (consultant)

EXTERNAL DISTRIBUTION

84–85. DOE DIVISION OR REACTOR RESEARCH AND DEVELOPMENT,
Washington, DC 20545

Director

86–88. DOE DIVISION OF WASTE MANAGEMENT, PRODUCTION AND REPROCESSING, Washington, DC 20545

Chief, Industrial Programs Branch
Chief, Projects Branch
Chief, Technology Branch

89–90. DOE OAK RIDGE OPERATIONS OFFICE, P.O. Box E, Oak Ridge, TN 37830

Director, Reactor Division
Director, Research and Technical Support Division

91–354. DOE TECHNICAL INFORMATION CENTER, Office of Information Services, P.O. Box 62, Oak Ridge, TN 37830

For distribution as shown in TID-4500 Distribution Category, UC-79b (Fuels and Materials Engineering Development); UC-79h (Structural Materials Design Engineering); UC-79k (Components)